Published in final edited form as:
Angew Chem Int Ed Engl. 2009 ; 48(31): 5642–5647. doi:10.1002/anie.200902028.

The True Structures of the Vannusals, Part 1: Initial Forays into Suspected Structures and Intelligence Gathering**

K. C. Nicolaou*, **H. Zhang**, and **A. Ortiz**

* Department of Chemistry and The Skaggs Institute for Chemical Biology, The Scripps Research Institute, 10550 North Torrey Pines Road, La Jolla, CA 92037 (USA) and Department of Chemistry and Biochemistry University of California, San Diego, 9500 Gilman Drive, La Jolla, CA 92093 (USA), Fax: (+1) (858) 784-2469, kcn@scripps.edu

Keywords

vannusals A & B; structural revision; total synthesis

Isolated from the tropical interstitial ciliate *Euplotes vannus* strains Si121 and BUN3, vannusals A and B were assigned structures **1** and **2**, respectively (Figure 1).[1,2] These novel and challenging molecular architectures fascinated scientists since their disclosure in 1999 and stood defiant to chemical synthesis until 2008, when we reported the first total synthesis of the originally assigned structure of vannusal B (**2**) and proved it to be wrong.[3] The puzzle of the correct structure of vannusal B was complicated by the scarcity of the natural product and its unprecedented carbon framework, leaving the challenge of its solution to chemical synthesis. In this and the following communication,[4] we report our investigations that led to the total synthesis of several suspected stereoisomers of this molecule and the eventual elucidation of its true structure (and that of its sibling, vannusal A) through its total synthesis.

Based on the interplay between total synthesis and NMR spectroscopy, the journey to the true structure of vannusal B was long and arduous. It became urgent and was initiated immediately upon completion of the total synthesis of its originally assigned structure (**2**).[3] In the following description, we unravel the logical evolution of events that led to the emergence of useful intelligence that allowed the eventual solution of the vannusal conundrum. Thus, on comparison of the NMR spectral data of natural vannusal B and synthetic **2**, it became apparent that the most striking differences were located in the "northeastern" region of the molecule, particularly around rings D and E. Strong NMR spectroscopic evidence (see Figure 2) indicated that stereocenters C_{26} (*w*-coupling, $JH_{26,15left}$ = 1.6 Hz; NOE, H_{26}/H_{27}) and C_{18} (NOE, H_{25}/H_{16}) were likely correct, leaving C_{25} and C_{21} as the most logical positions to start our structural modifications. This narrowed our choice to four diastereomeric structures, one of which (i.e. **2**) we had already synthesized.[3] From the remaining three, we selected the C_{21}-*epi* diastereomer of **2**, structure **3** (Figure 1), as our next target molecule based on a subtle and intriguing observation: that inversion of stereochemistry at C_{21} would bring the "northeastern" domain of vannusal B in line with the proposed biosynthetic hypothesis that postulated a

**We thank Professor Graziano Guella for samples and NMR spectra of vannusals A and B, and for helpful discussions. We also thank Drs. D. H. Huang, G. Siuzdak and R. Chadha for NMR spectroscopic, mass spectroscopic and X-ray crystallographic assistance, respectively. Financial support for this work was provided by the NSF (fellowship to A. Ortiz), the Skaggs Institute for Research, and a grant from the National Institutes of Health (USA).

Supporting information for this article is available on the WWW under http://www.angewandte.org or from authors.

dimerization of two identical monomeric units (prevannusal, naturally occurring)[2] as the biosynthetic precursors to vannusals A and B.

The strategy for the total synthesis of the targeted vannusal B diastereomer **3** relied on the retrosynthetic analysis outlined in Figure 3. Thus, based on our experience in the total synthesis of the originally assigned structure of vannusal B (**2**),[3] we dissected structure **3** at the indicated bonds through (a) a Li-mediated coupling reaction (C_{11}-C_{12}, originally as a C-C bond and eventually as a C=C bond), and (b) a SmI_2-based[5] cyclization (C_{10}-C_{28} bond). Accompanied by appropriate functional group modifications, these disconnections revealed vinyl iodide **5** and aldehyde **6** as potential key building blocks for the proposed construction.

With vinyl iodide (−)-**5** already in hand in its enantiopure form,[3] we proceeded to devise a synthesis for racemic aldehyde **6**, the other required fragment for the construction of structure **3**. This objective demanded different chemistry from that employed in the construction of its C_{21}-*epi* counterpart[3] used to synthesize the originally assigned vannusal B structure (**2**). Thus, and as shown in Scheme 1, epoxide **9** was synthesized through vanadium-catalyzed epoxidation [*t*BuOOH, $VO(acac)_2$ (cat.), 90 % yield] of homoallylic alcohol **8**, prepared from racemic **7**[3] by treatment with Martin's sulfurane (87 % yield). Epoxide **9** was formed as a single diastereomer through the exquisite stereocontrol exerted by the free homoallylic hydroxyl group within substrate **8**. The subsequent task of installing the intended nitrile moiety, through the use of the Nagata reagent (Et_2AlCN), however, required protection of this hydroxyl group as an acetate (Ac_2O, Et_3N, 4-DMAP, 90 % yield).[6] Upon exposure to Et_2AlCN, the latter compound afforded the targeted *trans* hydroxy nitrile **11**, as expected, in 81 % yield. Removal of the acetate group from **11** (K_2CO_3, MeOH) furnished the required dihydroxy nitrile **12,** in 100 % yield. The structure of **12** was secured unambiguously by X-ray crystalographic analysis[7] (see ORTEP drawing, Scheme 1) of its crystalline acetonide derivative **13** (mp 87–88 °C, hexanes) prepared by exposure of **12** to 2,2-dimethoxypropane in the presence of PPTS (cat.) (89 % yield) as shown in Scheme 1.

The elaboration of dihydroxy nitrile **12** to aldehyde **6** is summarized in Scheme 2. Thus, protection of the hydroxy groups of **12** with SEM moieties (SEMCl, iPr_2NEt, 90 % yield) led to bis–SEM derivative **14**, which was then converted to tertiary alcohol **15** through a four-step sequence [DIBAL-H reduction, MeMgBr addition, NMO-TPAP (cat.) oxidation, and MeMgBr addition, 72 % overall yield for four steps]. Capping the newly generated tertiary hydroxyl group within **15** required more forcing conditions (SEMCl, KHMDS, THF, −78→25 °C, 92 % yield), and led to the expected tri-SEM derivative **16**. The remaining steps to the desired aldehyde **6** followed our previously developed strategy[3] which required initial ozonolysis of **16** (89 % yield) and subsequent enolization/*O*-alkylation of the resulting aldehyde (KH, allyl chloride) to afford allyl enol ether **17** (91 % yield). Heating of the latter under μ–wave conditions (200 °C) effected the desired Claisen rearrangement, and $NaBH_4$ reduction converted the resulting aldehyde to the primary alcohol **18** (91 % overall yield for the two steps). Subsequent protection of the primary hydroxyl group within the latter (BOMCl, iPr_2NEt, nBu_4NI) followed by ozonolysis (O_3; Ph_3P) led to **19** (92 % overall yield for two steps), which was finally converted to (±)-**6** through silyl enol ether formation (DBU, TBSCl) and another ozonolysis (O_3; Ph_3P), in 92 % overall yield for the two steps.

With both key building blocks (−)-**5** and (±)-**6** in hand, we proceeded with their union and further elaboration of the desired diastereomeric coupling product to its final destination, vannusal B structure **3**, as shown in Scheme 3. Lithium–iodide exchange within (−)-**5** (*t*BuLi, THF, −78→ −40 °C) followed by addition of (±)-**6** led to two coupling products (ca. 1:1 *dr*), which, after removal of the TIPS group (TBAF, 25 °C), were chromatographically separated, providing **20** (41 % yield for two steps) and its diastereomer (**d**–**20**, not shown, 42 % yield for two steps). Diastereomer **20** was converted to cyclization precursor aldehyde carbonate **21**

through a four-step sequence involving temporary TES protection of the primary hydroxyl group (TESCl, imid.), installation of a carbonate moiety at C_{12} ($ClCO_2Me$, Et_3N), removal of the TES group [HF•py/py (1:4), 79 % over the three steps], and oxidation of the regenerated primary alcohol [$PhI(OAc)_2$-AZADO (cat.),[8] 95 % yield]. With precursor **21** at hand, we were then in a position to attempt the crucial SmI_2-induced ring closure reaction that would forge the entire carbon skeleton of our target molecule, a process whose efficiency and stereochemical outcome we found to be dependent on the nature of the protecting groups residing on the C_{26}, C_{25} and C_{22} oxygen residues, as well as the relative stereochemistry of the two domains of the molecule (i.e. **20** *vs* **d**-**20**). In this instance, the SEM groups on these positions in precursor **21** proved co-operative, facilitating its intended cyclization (SmI_2, HMPA, THF, − 10→25 °C) to afford two chromatographically separable diastereomers (**22β**, 33 % yield, **22α**, 21 % yield).[9] Both diastereomers could be easily converted into the same conjugated diene **23** through previously developed procedures[3] as a prelude to correcting their stereochemistry. Treatment of **22α** with $POCl_3$ and pyridine led to the formation of **23** in 72 % yield, while conversion of **22β** into **23** proceeded through a xanthate formation (NaH, CS_2; MeI) and Chugaev *syn*-elimination (microwave heating, 185 °C, 86 % yield for the two steps). Conjugated diene **23** was transformed regio- and stereoselectively to intermediate **24**, possessing the inverted and desired stereochemistry at C_{10} and C_{28}, by sequential hydroboration/oxidation ($ThexBH_2$; BH_3•THF; H_2O_2, 70 % yield) and phenylselenenylation/*syn* elimination (*o*$NO_2C_6H_4SeCN$, *n*Bu_3P; H_2O_2, 68 % overall yield). The final drive from **24** to vannusal B structure **3** proceeded through intermediate **25** (Scheme 3) and required installment of a TES group at C_{28} (TESCl, KHMDS, 89 % yield), removal of the BOM groups (LiDBB, 83 % yield), selective oxidation of the primary alcohol over the secondary [$PhI(OAc)_2$, 1-Me-AZADO (cat.)],[8] acetylation (Ac_2O, 4-DMAP, 87 % yield for two steps), and, finally, aq. HF-induced global deprotection [aq. HF:THF (1:3), 77 %]. The AZADO and 1-Me-AZADO catalysts[8] (see structures, Scheme 3) proved to be superior to TEMPO in these studies, and were subsequently employed with success in several other sequences instead of the latter. Although consistent with its structure, the NMR spectroscopic data of synthetic vannusal B structure **3** did not match those reported for the natural product, sending us back to the drawing board to contemplate our next move. Disappointing as they were, these data, however, pointed to a new line of investigation. Specifically, the rather large coupling constant between H_{25} and H_{21} ($JH_{25,\,21}$ = 8.5 Hz, see Figure 4) exhibited in the ^1H NMR spectrum of **3** (a C_{25}/C_{21} trans structure) seemed to suggest that the true structure of vannusal B (exhibiting $JH_{25,\,21}$ = 1.6 Hz) possessed a C_{25}/C_{21} *cis* arrangement rather than a *trans* relationship.

Having excluded structure **3** [C_{21}-*epi*-**2**] as the true structure of vannusal B, we then moved to our second target, diastereomer **4** [C_{21}-*epi*, C_{25}-*epi*-**2**], possessing a C_{25}/C_{21} *cis* relationship, as a possibility for the coveted vannusal B structure. The required aldehyde building block **30** for this construction was synthesized from diketone **26**[3] as summarized in Scheme 4. Thus, lithium enolate generation from **26** (LDA, −78→−40 °C) followed by addition of acetone led to a diastereomeric mixture of aldol products in which the β-stereoisomer was predominating (ca. 3:1 *dr*). TES protection (TESOTf, 2,6-lut.) followed by chromatographic separation furnished isomerically pure diketone **27** (66 % overall yield for the two steps), which was selectively reduced from the α-face with $NaBH_4$ (THF:MeOH, 1:1, −10→25 °C) at both carbonyl sites to afford, after removal of the TES group (PPTS, EtOH), triol **28** in 91% yield. Regioselective acetonide formation within the latter intermediate [$(MeO)_2CMe_2$, PPTS, 100 % yield], followed by SEM installation (SEMCl, *i*Pr_2NEt, *n*Bu_4NI, 97 % yield] led to intermediate **29**. The latter was converted to the desired aldehyde, (±)-**30**, by the same route and in similar yields, as the one described above for the conversion of **16** to (±)-**6** (see Scheme 2), as summarized in Scheme 4.

The total synthesis of vannusal B diastereomeric structure **4** [C_{21}-*epi*, C_{25}-*epi*-**2**] from (−)-**5** and (±)-**30** proceeded through similar intermediates and along the same lines as the route to vannusal B structure **3** [C_{21}-*epi*-**2**] from (−)-**5** and (±)-**6** discussed above (see Scheme 3). Notable differences between the two routes were the higher yield obtained in the SmI_2-mediated ring closure step (74 %), which was most likely a consequence of the use of the acetonide moiety at the C_{25}/C_{21} site, and the isolation of only one diastereomer at this stage, that corresponding to **22β** (Scheme 3). Again, the NMR spectroscopic data of synthetic structure **4** were disappointing in that they did not match those of the natural vannusal B. However, we were encouraged by the ^{1}H NMR spectrum of this structure, which revealed much closer chemical shifts for H_{17} and H_{26} (δH_{17} = 2.50; δH_{26} = 4.05 ppm) to those exhibited by the natural product (δH_{17} = 2.48 ppm; δH_{26} = 3.95 ppm), than the originally assigned structure **2**, whose chemical shifts for these protons were far from close (δH_{17} = 2.24 ppm; δH_{26} = 4.53 ppm) to those of the natural product (see Figure 5). Based on these observations, we surmised that the "northeastern" domain (i.e. ring E) of the true structure of vannusal B possessed the stereochemistry shown in structure **4** with the *cis* C_{25}/C_{21} stereochemical arrangement (Figure 1). At this point, we turned our attention to the "southwestern" part of the molecule (i.e. ring A), aiming at stereochemical changes in that region to define our next targets.

Careful consideration of the reported ^{1}H NMR spectral data of both vannusals A and B led us to believe that the relative stereochemistry at C_6 with regards to C_3, C_{29}, and C_7 of the originally assigned structures of the vannusal (**1**, see Figure 6a) was correct. This assumption was based on a) the rather large ^{1}H NMR coupling constant between H_6 and H_7 ($JH_{6,7}$ = 10.0 Hz), which supported the assigned *trans*-diaxial orientation of these two protons, and b) the observed NOEs between H_{29} and $H_{8\beta}$, and $H_{5\alpha}$ and H_{12} (see Figure 6a). Indeed, the 6-*epi* diastereomer of **2** (not shown) is problematic in that it cannot accommodate these observations as supported by model system **31e**[10] (Figure 6c), which exhibits rather similar ^{1}H NMR coupling constants between H_6 and H_7 ($JH_{6,7}$ = 12.0 Hz), H_6 and H_{29} ($JH_{6,29}$ = 3.5 Hz), and H_3 and H_{29} ($JH_{3,29}$ = 3.5 Hz) as those exhibited by the natural product ($JH_{6,7}$ = 10.0 Hz; $JH_{6,29}$ = 3.5 Hz; $JH_{3,29}$ = 3.5 Hz), but no NOE between H_{29} and neither of the two H_8 protons. This conclusion left C_3 and C_{29} as the possible sites of structural misassignment in the original report.[1] In order to elucidate this point, we synthesized all four possible diastereomers of the model AB ring system (compounds **31a**–**31d**),[10] Figure 6b) and compared their NMR spectral data with those of the natural vannusal A. While all four model systems exhibited the expected NOEs between H_{29} and $H_{8\beta}$, their ^{1}H NMR chemical shifts and coupling constants of H_{29} were revealing (**31a**: δ = 5.43 ppm, $JH_{29,3}$ = 3.5 Hz, $JH_{29,6}$ = 3.5 Hz; **31b**: δ = 5.22 ppm, $JH_{29,3}$ = 7.8 Hz, $JH_{29,6}$ = 7.8 Hz; **31c**: δ = 5.29 ppm, $JH_{29,3}$ = 4.5 Hz, $JH_{29,6}$ = 2.0 Hz; **31d**: δ = 5.30 ppm, $JH_{29,3}$ = 1.8 Hz, $JH_{29,6}$ = 5.4 Hz) (see Figure 6b). Indeed, the striking resemblance of the ^{1}H NMR spectral data of model system **31a** (as opposed to the other three) to those reported for the natural vannusal A (δ = 5.43 ppm, $JH_{29,3}$ = 3.5 Hz, $JH_{29,6}$ = 3.5 Hz) were convincing of the correctness of the originally assigned configurations at C_3, C_{29}, C_6 and C_7 of the molecule. It was through this pathpointing intelligence that we returned back to the most "northeastern" ring of the vannusal structure to contemplate the remaining possibilities. In the following communciation, we unravel our next course of action and the events that led to the total synthesis of the true structure of vannusal B, and thereby, the elucidation of its molecular architecture, and that of its sibling, vannusal A.

Supplementary Material

Refer to Web version on PubMed Central for supplementary material.

References

1. Guella G, Dini F, Pietra F. Angew Chem 1999;111:1217–1220.Angew Chem Int Ed 1999;38:1134–1136.
2. Guella G, Callone E, Di Giuseppe G, Frassanito R, Frontini FP, Mancini I, Dini F. Eur J Org Chem 2007:5226–5234.
3. Nicolaou KC, Zhang H, Ortiz A, Dagneau P. Angew Chem 2008;120:8733–8738.Angew Chem Int Ed 2008;47:8605–8610.
4. Nicolaou KC, et al. Angew Chem. 2009submittedAngew Chem Int Ed. 2009submitted, see following communication in this issue
5. For reviews on samarium diiodide used in organic synthesis, see: a) Edmonds DJ, Johnston D, Procter DJ. Chem Rev 2004;104:3371–3403. [PubMed: 15250745] b) Kagan HB. Tetrahedron 2003;59:103510–10372. c) Molander GA, Harris CR. Chem Rev 1996;96:307–308. [PubMed: 11848755]
6. Reaction of hydroxy epoxide 9 with Et_2AlCN resulted in the predominant transfer of an Et group to the substrate rather than a CN group, presumably through initial formation of the $–OAlEt_2$ species (C_{26}) followed by intramolecular epoxide activation and delivery of an Et group.
7. CCDC–726953 contains the supplementary crystallographic data for 13 and is available free of charge from The Cambridge Crystallographic Data Centre via www.ccdc.cam.ac.uk/data_request/cif
8. Shibuya M, Tomizawa M, Suzuki I, Iwabuchi Y. J Am Chem Soc 2006;128:8412–8413. [PubMed: 16802802]We thank Professor Iwabuchi and Nissan Chemical Industries, Ltd. for generous gifts of AZADO and 1-MeAZADO catalysts
9. Despite the modest yield, this reaction served us well given the failure of the originally employed C_{25}/C_{26} acetonide, C_{21}–SEM precursor to give any cyclization product under the same conditions.
10. Details of these syntheses will be reported in the full account of this work, selected physical properties of compounds 31a–31e are given in the Supporting Information.

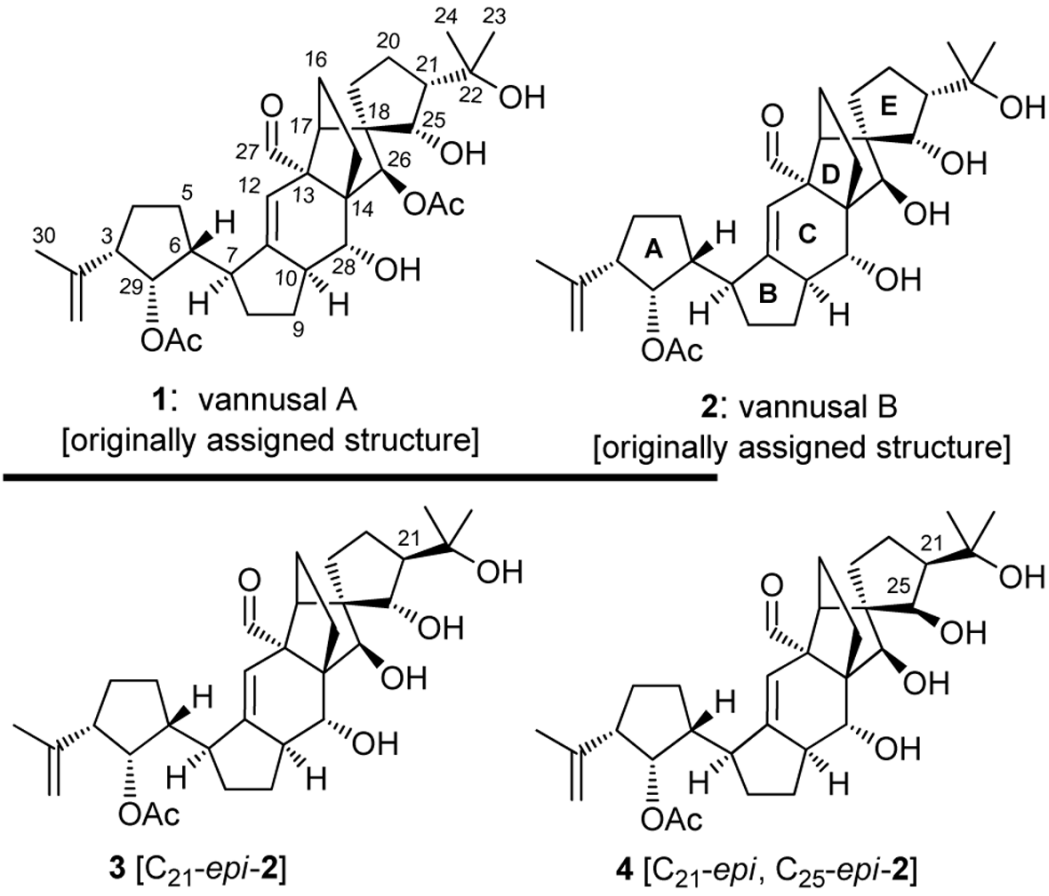

Figure 1.
Originally assigned structures of vannusals A (**1**) and B (**2**) and initially targeted stereoisomers **3** [C_{21}-*epi*-**2**] and **4** [C_{21}-*epi*, C_{25}-*epi*-**2**].

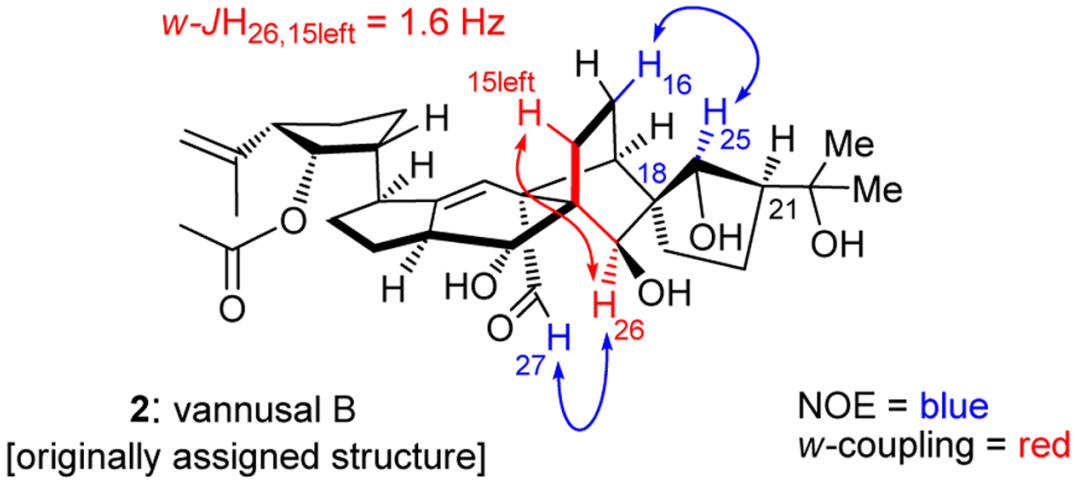

Figure 2.
Key ^{1}H NMR coupling constant (w-$JH_{26,\ 15left}$ = 1.6 Hz) and NOE exhibited by both the originally assigned structure (synthetic, **2**) and natural vannusal B.

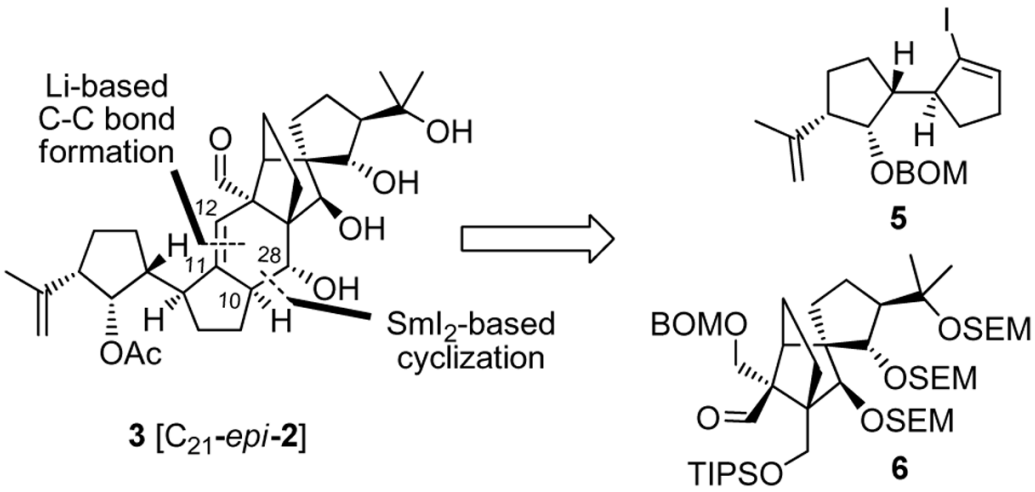

Figure 3.
Retrosynthetic analysis of vannusal B stereoisomer **3** [C_{21}-*epi*-**2**]. BOM = benzyloxymethyl; SEM = trimethylsilylethoxymethyl; TIPS = triisopropylsilyl.

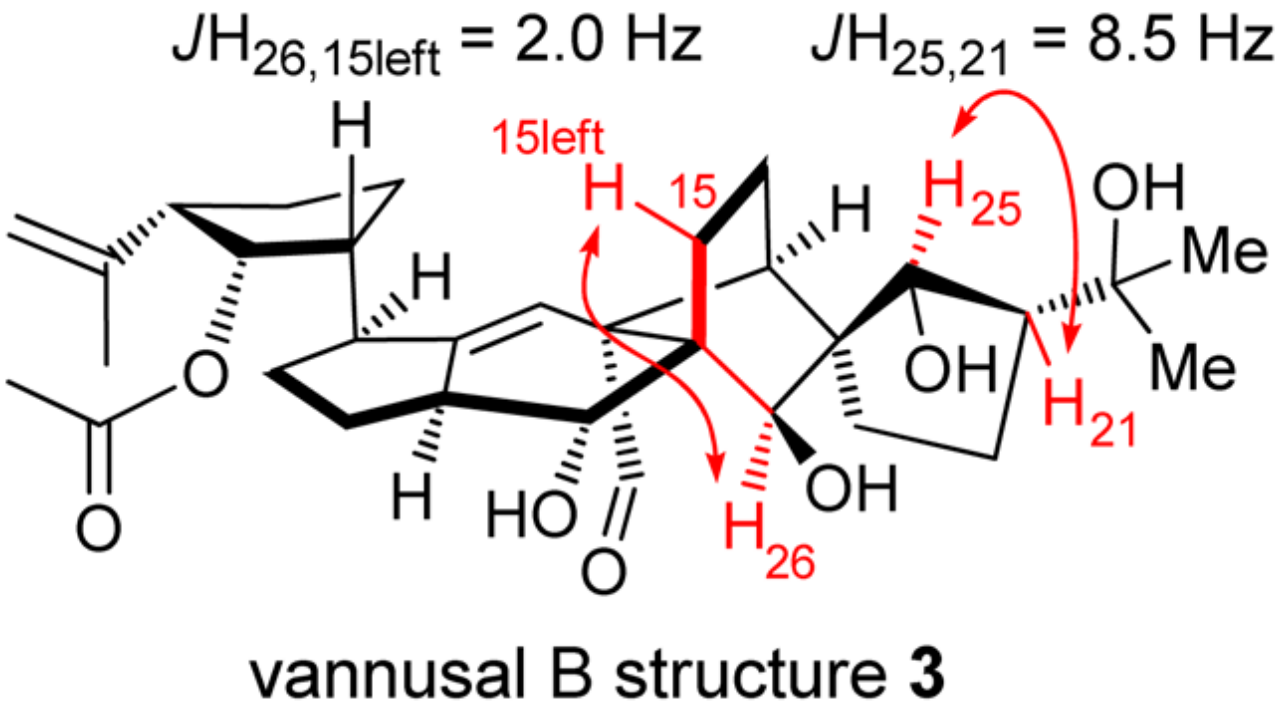

Figure 4.
Key ^{1}H NMR coupling constants of vannusal B structure **3** ($JH_{25,21}$ = 8.5 Hz, *w*-$JH_{26,15left}$ = 2.0 Hz)

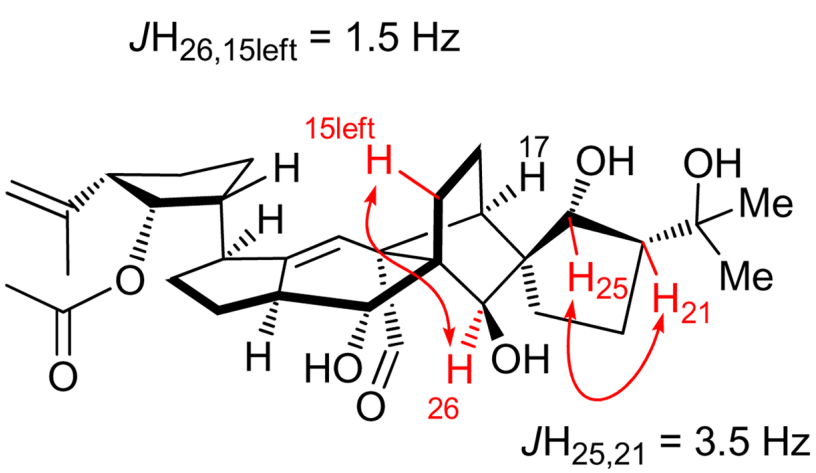

^{1}H NMR chemical shift (ppm)			
cpd[a]	H_{17}	H_{25}	H_{26}
4	2.50	4.41	4.05
nvB[b]	2.48	4.37	3.95
2	2.25	4.53	4.40

[a]**cpd**: compound
[b]**nvB**: natural vannusal B

Figure 5.
Key ^{1}H NMR coupling constants (*w*-$JH_{26,\ 15left}$ = 1.5 Hz, $JH_{25,\ 21}$ = 3.5 Hz) and selected chemical shifts for vannusal B structure **4** and comparisons with those of natural vannusal B and its originally assigned structure (**2**).

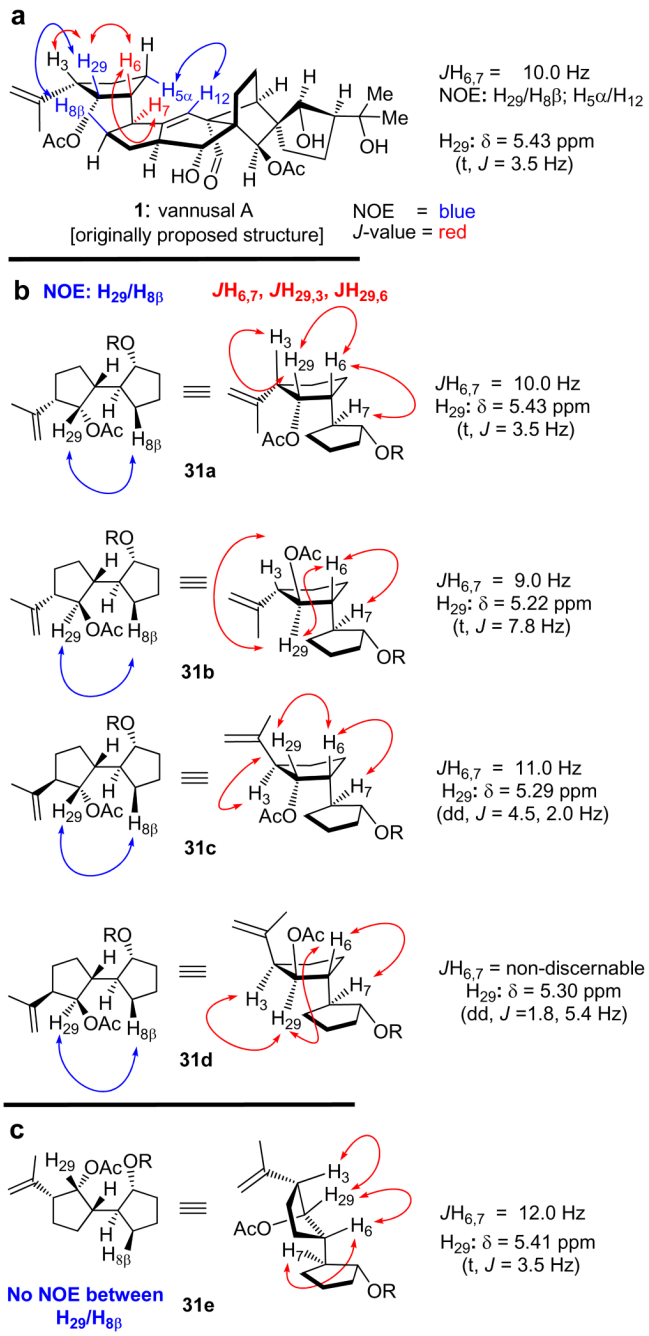

Figure 6.

Relevant NOE's and coupling constants (*J*) of AB ring model compounds **31a**–**31e**. R =TBDPS = *tert*-butyldiphenylsilyl.

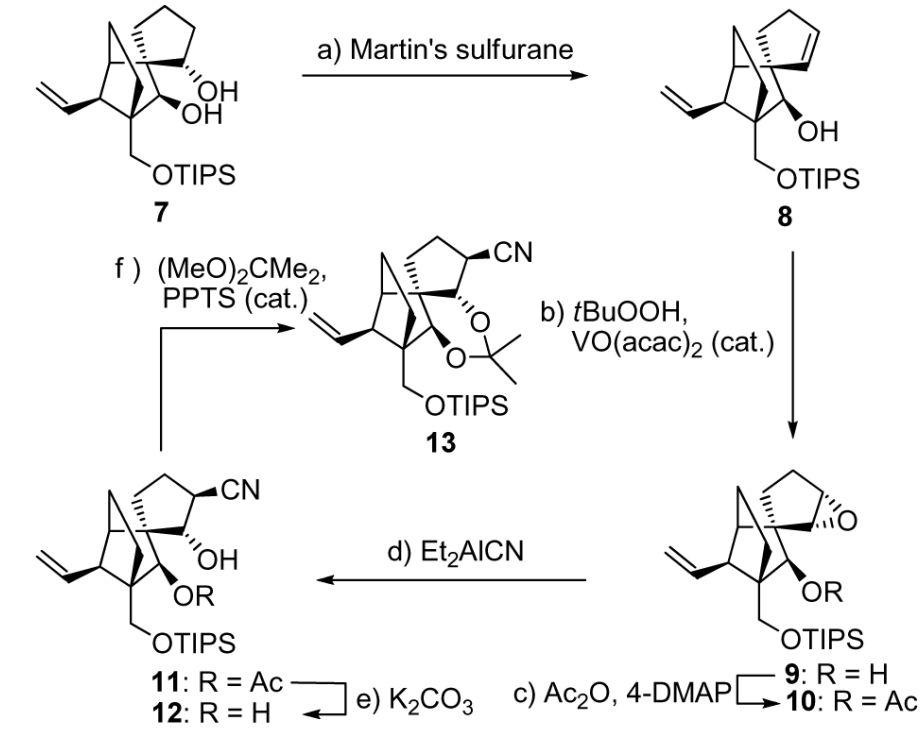

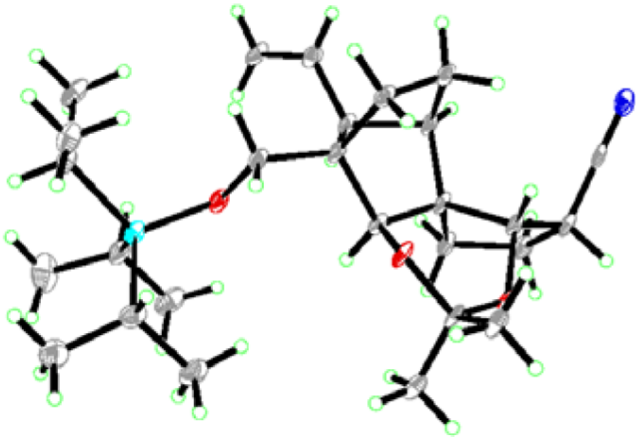

ORTEP drawing of **13**

Scheme 1.

Construction of nitrile **12** (top) and X-ray derived ORTEP drawing of **13** (bottom). Reagents and conditions: (a) Martin's sulfurane (1.1 equiv), Et_3N (10 equiv), CH_2Cl_2, 25 °C, 5 h, 87 %; (b) *t*BuOOH (3.0 equiv), $VO(acac)_2$ (0.2 equiv), PhH, 25 °C, 6 h, 90 %; (c) Ac_2O (10 equiv), Et_3N (30 equiv), 4-DMAP (1.0 equiv), CH_2Cl_2, 4 h, 25 °C, 90 %; (d) Et_2AlCN (10 equiv), PhMe, −78→−20 °C, 19 h, 81 %; (e) K_2CO_3 (1.0 equiv), MeOH, 25 °C, 2 h, 100 %; (f) DMF/2,2-dimethoxypropane (1:1), PPTS (1.0 equiv), 24 h, 89 %.

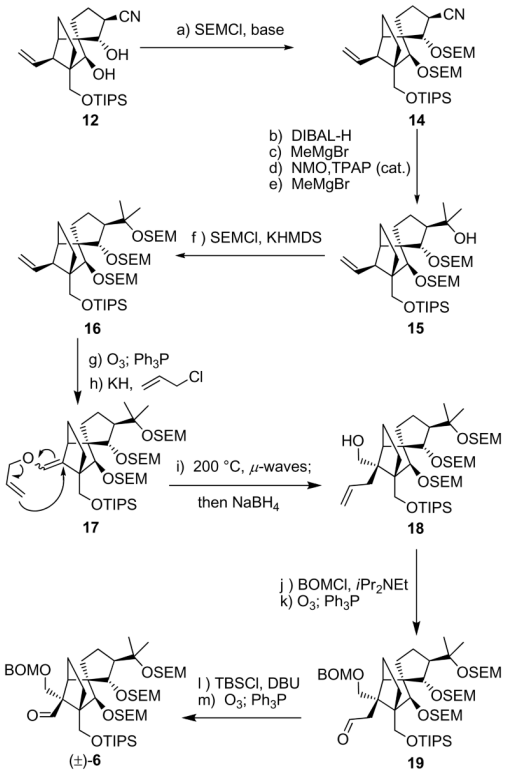

Scheme 2.

Construction of aldehyde (±)-**6**. Reagents and conditions: (a) SEMCl (10 equiv), *i*Pr_2NEt (30 equiv), CH_2Cl_2, 50 °C, 48 h, 90 %; (b) DIBAL-H (1.1 equiv), PhMe, −78→30 °C, 1 h; then 0.1 M HCl, 25 °C, 20 min; (c) MeMgBr (10 equiv), THF, 0 °C, 30 min; (d) NMO (2.0 equiv), TPAP (0.05 equiv), CH_2Cl_2/CH_3CN (7:1), 25 °C, 3 h; (e) MeMgBr (10 equiv), THF, −10 °C, 20 min, 72 % for four steps; (f) KHMDS (2.0 equiv), SEMCl (5.0 equiv), Et_3N (10 equiv), 1 h, 92 %; (g) O_3, py (1.0 equiv), CH_2Cl_2:MeOH (1:1), −78 °C; then Ph_3P (5.0 equiv), −78→25 °C, 1 h, 89 %; (h) KH (10 equiv), allyl chloride (30 equiv), HMPA (10 equiv), DME, 25 °C, 12 h, 91 %; (i) *i*Pr_2NEt (1.0 equiv), *o*-dichlorobenzene, 200 °C (μ-waves), 20 min; then $NaBH_4$ (10 equiv), MeOH, 1 h, 25 °C, 91 % for two steps; (j) BOMCl (10 equiv), *i*Pr_2NEt (30 equiv), *n*Bu_4NI (1.0 equiv), CH_2Cl_2, 50 °C 12 h; (k) O_3, py (1.0 equiv), CH_2Cl_2:MeOH (1:1), −78 °C; then Ph_3P (5.0 equiv), − 78→25 °C, 1 h, 92 % for two steps; (l) TBSCl (10 equiv), DBU (20 equiv), CH_2Cl_2, 25 °C, 48 h; (m) O_3, py (1.0 equiv), CH_2Cl_2:MeOH (1:1), −78 °C; then Ph_3P (5.0 equiv), −78→25 °C, 1 h, 92 % for two steps. HMPA = hexamethylphosphoramide, DBU = 1,8-diazoicyclo[5.4.0]undec-7-ene.

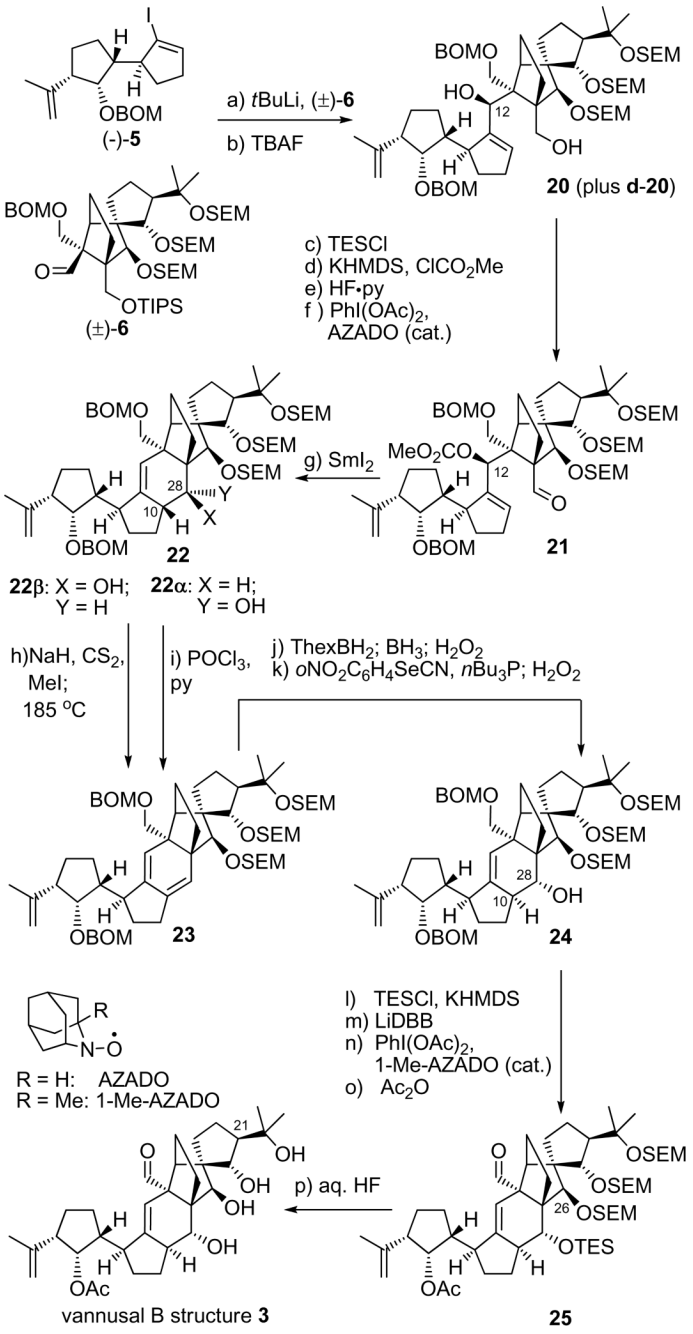

Scheme 3.

Synthesis of vannusal B structure **3** [C_{21}-*epi*-**2**]. Reagents and conditions: (a) (−)-**5** (1.3 equiv), *t*BuLi (2.5 equiv), THF, −78→−40 °C, 50 min; then (±)-**6** (1.0 equiv), −40→0 °C, 20 min; (b) TBAF (2.0 equiv), THF, 25 °C, 6 h, **20**, 41% for two steps, **d-20**, 42 % for two steps; (c) TESCl (2.0 equiv), imid (10 equiv), CH_2Cl_2, 25 °C, 5 h; (d) KHMDS (5.0 equiv), $ClCO_2Me$ (10.0 equiv), Et_3N (10 equiv), THF, −78→25 °C, 1 h; (e) HF•py/py (1:4), 0→25 °C, 12 h, 79 % for three steps; (f) $PhI(OAc)_2$ (2.0 equiv), AZADO (0.1 equiv), CH_2Cl_2, 25 °C, 24 h, 95 %; (g) SmI_2 (0.1 M in THF, 4.0 equiv), HMPA (12 equiv), THF, −20→25 °C, 3.5 h, **22β**, 33 % yield, **22α**, 21 %; (h) NaH (15 equiv), CS_2 (30 equiv), THF, 0→25 °C, 30 min; then MeI (45 equiv), 25 °C, 24 h; then 185 °C, μ-waves), *o*-dichlorobenzene, 15 min, 86 % for two steps; (i)

$POCl_3$, pyridine, 72 % (j) $ThexBH_2$ (5.0 equiv), THF, − 10→25 °C, 0.5 h; then BH_3•THF (15 equiv), 25 °C, 1 h; then 30 % H_2O_2/3 N NaOH (1:1 *dr*), 0→45 °C, 1 h; 70 %; (k) *o*$NO_2C_6H_4SeCN$ (3.0 equiv), *n*Bu_3P (6.0 equiv), py (9.0 equiv), THF, 25 °C; then 30 % H_2O_2, 0→45 °C, 68 %; (l) KHMDS (6.0 equiv), TESCl (4.0 equiv), Et_3N (8.0 equiv), THF, −50→25 °C, 30 min, 89 %; (m) LiDBB (excess), THF, −78→−50 °C, 1 h, 83 %; (n) PhI $(OAc)_2$ (2.0 equiv), 1-Me-AZADO (0.2 equiv), CH_2Cl_2, 25 °C, 22 h; (o) Ac_2O (30 equiv), Et_3N (90 equiv), 4-DMAP (2.0 equiv), CH_2Cl_2, 25 °C, 36 h, 87 % for two steps; (p) 48 % aq. HF:THF (1:3), 25 °C, 7 h, 77 %. KHMDS = potassium hexamethyldisilyazide, Thexyl = thexylborane, LiDBB = Lithium di-*tert*-butylbiphenyl.

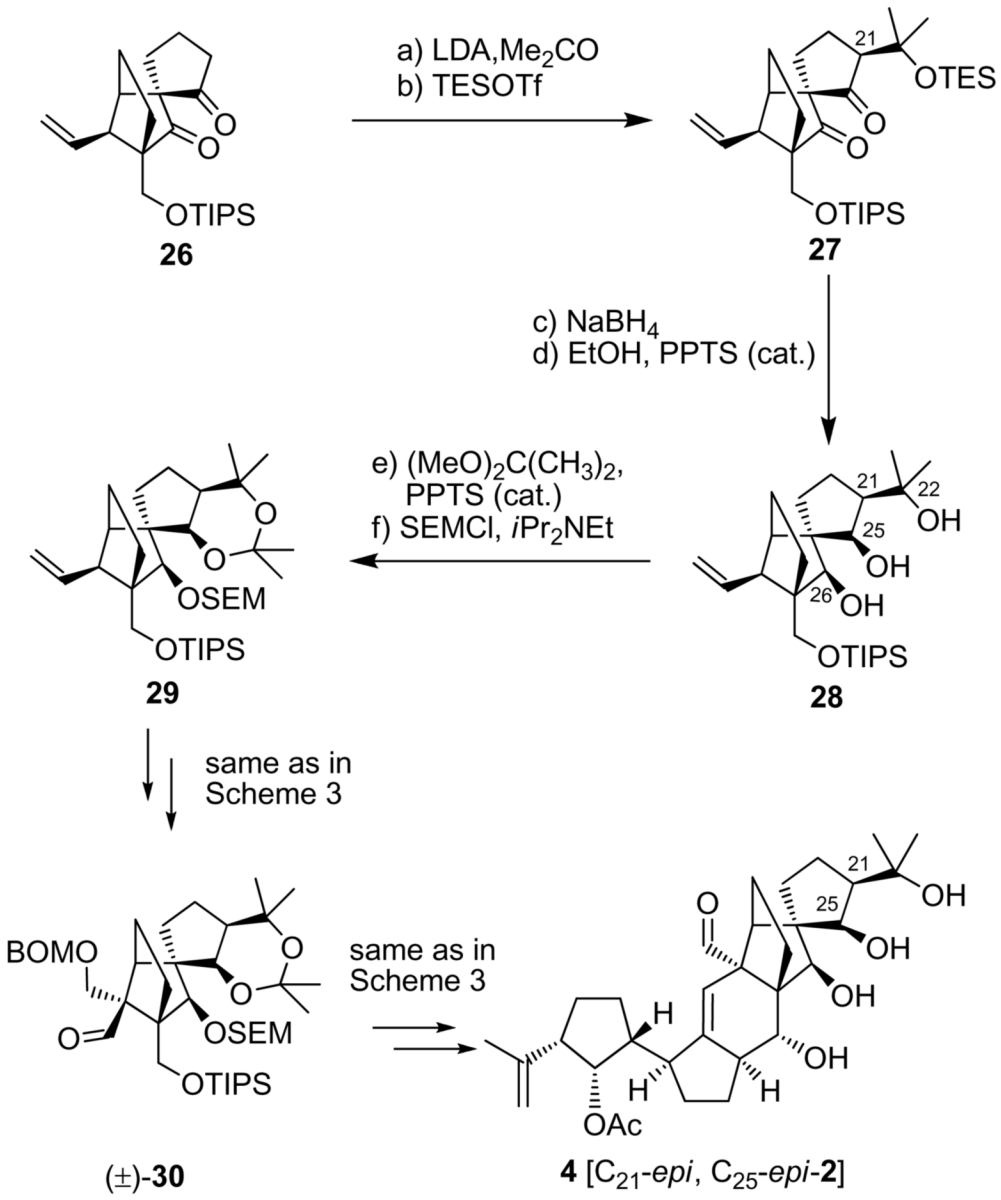

Scheme 4.

Synthesis of aldehyde (±)-**30** and vannusal B structure **4**. Reagents and conditions: (a) LDA [generated from *i*Pr_2NH (5.0 equiv), *n*BuLi (2.5 M in haxanes, 5.0 equiv)], THF, −78→−40 °C; then acetone (20 equiv), −40→25 °C, 1 h, (3:1 *dr*); (b) TESOTf (2.0 equiv), 2,6-lut. (5.0 equiv), −78→−40 °C, 1 h, 66 % for two steps; (c) $NaBH_4$ (20 equiv), THF:MeOH (1:1), −10→25 °C, 4 h; (d) EtOH, PPTS (0.10 equiv), 25 °C, 2 h, 91 % for two steps; (e) $(MeO)_2C(Me)_2$:DMF (1:1), PPTS (1.0 equiv), 25 °C, 48 h, 100 %; (f) SEMCl (5.0 equiv), *i*Pr_2NEt (15 equiv), *n*Bu_4NI (1.0 equiv), CH_2Cl_2, 50 °C, 24 h, 97 %;